MRI Provides More Accurate Renal Motion Estimation than 4D-CT for Radiation Treatment Planning in Young Children

Adam M Winchell[1,2], Atmaram Pai Panandiker[1], Ruitian Song[1], Ralf B Loeffler[1], and Claudia M Hillenbrand[1]

[1]*Radiological Sciences, St. Jude Children's Research Hospital, Memphis, TN, United States,* [2]*Biomedical Engineering, University of Memphis, Memphis, TN, United States*

Target Audience: Those interested in motion tracking, especially for abdominal radiation treatment planning

Introduction: Neuroblastoma (NB) is a common extra-cranial, sympathoadrenal solid tumor of the pediatric population with a notably poor prognosis. During the past two decades, emphasis has been placed on systemic therapy because the majority of children present with metastatic disease. As systemic tumor control improves, the proportion of patients who experience primary site failure has increased.[1,2] This has prompted re-examination of loco-regional tumor control with intensity-modulated radiation therapy (IMRT) to provide dose-escalation with the goal to improve overall survival. Appropriate delivery of IMRT within the abdomen requires precise temporospatial definition of the target and surrounding normal tissue. This reduces normal tissue dose and associated complications related to radiation exposure,[3] while simultaneously increasing dose delivered to target tissues. 4D-CT is usually used to measure abdominal organ motion.[4] However, kidney-to-liver contrast is poor and patients are exposed to ~8x the dose of a diagnostic CT scan.[4] To test whether real-time MRI could be as an alternative tracking approach, we measured respiratory induced kidney motion in young children with abdominal NB using both, 4D-CT and real-time-MRI, and evaluated tracking accuracy.

Methods: Eight children (male=3; female=5; mean age=4.9y) diagnosed with high-risk abdominal NB have been enrolled in an ongoing IRB approved prospective study to estimate local control and pattern of disease recurrence when treated with IMRT. Each patient received a 4D-CT and real-time MRI in treatment position to assess respiratory induced renal motion. The 4D-CT (Somatom Sensation Open, Siemens Medical Solutions) scan consisted of axial slices ($0.53x0.53x3.00mm^3$) covering the abdomen with the following parameters: 400 effective mA, 120kV, 0.5-1s gantry rotation, 0.1 pitch, 1.2mm collimation. The images were binned into 8 positions according to a respiratory trace from a pressure-sensitive Anzai belt (Anzai Medical). The real-time MRI at 1.5T (Magnetom Avanto, Siemens Medical Solutions) consisted of 200 TrueFISP images acquired consecutively in a single coronal slice covering both kidneys and a sagittal slice for each kidney (T_{AQ} 546ms, TE 2.1ms, pixel size (1.1-1.6)x(1.1-1.6) mm^2, slice thickness 7mm, matrix 128x128, duration 1:49min per data set). Coronal images were used to determine superior/inferior (SI) and medial/lateral (ML) physiologic motion, and sagittal image data sets for anterior/posterior (AP) motion. Physiologic motion was measured in real-time MRI and 4D-CT by tracing user defined extreme points on the kidney boundary (i.e. top, bottom, etc., see Figure 1) in a custom graphical user interface written in MATLAB.

Results: An example of typical soft tissue contrast of the liver and kidney achieved with CT and MRI is shown in Figure 1. The isodense kidneys in the CT images decreased the ability to differentiate kidney borders for physiological motion tracking, especially in these post-operatively primary adrenal tumors conditions. The measured motion in each of the eight patients by 4D-CT and real-time MR is presented in Table 1. Two patients had a non-representatively normal kidney (patient 4 = malrotated right kidney in pelvis; patient 5 = severely atrophic left kidney) and were removed from the motion analysis. The largest renal motion was observed in SI direction. In nine of 14 kidneys (64%), MR measured SI motion smaller than the spatial resolution of CT (3mm). In ML and AP direction, the average motion measured was less than 1mm.

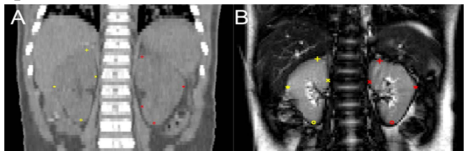

Figure 1: *(A) 4D-CT has poor kidney contrast in this coronal re-sliced image to track SI and ML organ motion. (B) Real-time MRI has superior kidney contrast to track organ motion in this coronal image. The yellow and red tracking points indicate sampling sites of motion.*

Table 1: *Left and right kidney organ motion measured in 8 patients using real-time-MRI and 4D-CT. Motion estimates are in mm (voxel size).*

Right Kidney

			Superior		Inferior		Anterior		Posterior		Medial		Lateral	
Patient	Gender	Age(Y)	CT	MR	CT	MR	CT	MR	CT	MR	CT	MR	CT	MR
1	F	2.08	3(3)	3.2(1.6)	3(3)	3.2(1.6)	0(0.59)	1.6(1.6)	1.18(0.59)	1.6(1.6)	0.59(0.59)	1.6(1.6)	0.59(0.59)	1.6(1.6)
2	F	1.64	3(3)	1.4(1.4)	3(3)	1.4(1.4)	0(0.59)	0(1.4)	0(0.59)	0(1.4)	0(0.59)	0(1.4)	0(0.59)	1.4(1.4)
3	M	2.79	3(3)	2.8(1.4)	0(3)	2.8(1.4)	1.18(0.59)	0(1.2)	0.59(0.59)	0(1.2)	0(0.59)	0(1.4)	0(0.59)	0(1.4)
4	M	7.78												
5	F	10.25	6(3)	4(2)	3(3)	4(2)	0.59(0.59)	2(2)	0.59(0.59)	0(2)	0.59(0.59)	0(2)	1.18(0.59)	2(2)
6	M	4.64	3(3)	1.6(1.6)	0(3)	1.6(1.6)	0(0.59)	0(1.4)	0(0.59)	0(1.4)	0(0.59)	0(1.6)	0.59(0.59)	1.6(1.6)
7	F	5.64	3(3)	3.12(1.04)	3(3)	2.08(1.04)	1.18(0.59)	0(1.25)	0.59(0.59)	0(1.25)	0(0.59)	0(1.04)	0.59(0.59)	0(1.04)
8	F	4.41	3(3)	2.5(1.25)	3(3)	2.5(1.25)	0.59(0.59)	1.25(1.25)	0(0.59)	0(1.25)	0.59(0.59)	1.25(1.25)	0(0.59)	0(1.25)
		mean±std	3.4±1.1	2.7±0.9	2.1±1.5	2.5±0.9	0.5±0.5	0.7±0.9	0.4±0.4	0.2±0.6	0.3±0.3	0.4±0.7	0.4±0.4	0.9±0.9

Left Kidney

			Superior		Inferior		Anterior		Posterior		Medial		Lateral	
Patient	Gender	Age(Y)	CT	MR	CT	MR	CT	MR	CT	MR	CT	MR	CT	MR
1	F	2.08	3(3)	3.2(1.6)	3(3)	3.2(1.6)	0(0.59)	1.6(1.6)	0.59(0.59)	1.6(1.6)	0.59(0.59)	1.6(1.6)	0.59(0.59)	1.6(1.6)
2	F	1.64	0(3)	1.4(1.4)	0(3)	1.4(1.4)	0.59(0.59)	0(1.4)	0(0.59)	0(1.4)	0(0.59)	0(1.4)	0(0.59)	0(1.4)
3	M	2.79	0(3)	2.8(1.4)	3(3)	2.8(1.4)	0.59(0.59)	0(1.2)	0.59(0.59)	0(1.2)	0(0.59)	1.4(1.4)	1.18(0.59)	0(1.4)
4	M	7.78	3(3)	1.3(1.3)	6(3)	1.3(1.3)	1.18(0.59)	0(0.94)	0.59(0.59)	0(0.94)	0.59(0.59)	0(1.3)	0(0.59)	0(1.3)
5	F	10.25												
6	M	4.64	3(3)	1.6(1.6)	0(3)	1.6(1.6)	0(0.59)	0(1.4)	0(0.59)	0(1.4)	0(0.59)	0(1.6)	0.59(0.59)	0(1.6)
7	F	5.64	3(3)	3.12(1.04)	3(3)	3.12(1.04)	0.59(0.59)	0(1.25)	0.59(0.59)	0(1.25)	0.59(0.59)	0(1.04)	1.77(0.59)	1.04(1.04)
8	F	4.41	3(3)	2.5(1.25)	3(3)	2.5(1.25)	0.59(0.59)	0(1.25)	0(0.59)	0(1.25)	0.59(0.59)	0(1.25)	0(0.59)	0(1.25)
		mean±std	2.1±1.5	2.3±0.8	2.6±2.1	2.3±0.8	0.5±0.4	0.2±0.6	0.3±0.3	0.2±0.6	0.3±0.3	0.4±0.7	0.6±0.7	0.4±0.7

Discussion/Conclusion: Real-time MRI provides better tissue contrast of the kidney and about two time higher spatial resolution in the SI direction compared to 4D-CT enabling superior demarcation of organ boundaries and anatomical tracking. This clearly improves overall tracking accuracy. In the majority of kidneys, the SI motion measured by MR was less than the spatial resolution of CT (3mm). This indicates that CT is limited in its effectiveness to measure kidney motion in this population. MR is not dependent upon an external belt to accurately represent a respiratory cycle. This inherently makes MR less prone to external factors like data error (binning error) and belt positioning. MR also collects motion traces over multiple respiratory cycles increasing the confidence of the motion estimate. As a result, real-time MR provided the necessary spatiotemporal resolution to aid in highly conformal treatment planning for IMRT and proton therapy in a young patient population. Real-time MRI would eliminate the additional ionizing radiation doses resulting from the 4D-CT, and thereby reduce cumulative lifetime radiation dose to these young patients. With less than six minutes of total imaging time, the addition of this kidney motion protocol can be easily added to any baseline MR imaging scan with minimal disruption and would completely eliminate the need of a 4D-CT scan and associated ionizing radiation dose.

References: [1] George RE, *et al*. (2006) J Clin Oncol; 24(18):2891-96. [2] Wolden SL, *et al*. (2004) Intl J Rad Onc Bio Phys; 46(4): 969-74. [3] Bolling T, *et al*. (2010) Anticancer Res; 30:227-231. [4] Pai Panandiker AS, *et al*. (2012) Intl J Rad Onc Bio Phys; 82(5):1771-6.